Noise Figure in Near-Infrared Amorphous and Mid-Infrared Crystalline Silicon Optical Parametric Amplifiers

Jichi Ma and Sasan Fathpour, *Senior Member, IEEE*

***Abstract*—The noise figures (NF) of near-infrared (near-IR) amorphous silicon (a-Si) and mid-infrared (mid-IR) crystalline silicon (c-Si) optical parametric amplifiers (OPA) are numerically investigated. The impact of nonlinear losses, i.e., two-photon absorption (TPA) and TPA-induced free carrier absorption (FCA), as well as Raman-effect-induced complex nonlinear coefficient are taken into account in a-Si OPAs. The amplified spontaneous emission (ASE) of Erbium-doped fiber amplifiers (EDFA) and the relative intensity noise (RIN) of the pump laser are considered as the dominant pump noises when simulating the pump transferred noise (PTN) of near-IR a-Si and mid-IR c-Si OPAs, respectively. It is shown that in typical near-IR a-Si OPAs, the NF is ∼5 dB on the Stokes side but increases sharply to above 10 dB at the gain edge on the anti-Stokes side. In high-gain mid-IR c-Si OPAs, the NF is dominated by the PTN and is well above 10 dB at the gain edge. These results indicate that both near-IR a-Si OPAs and mid-IR c-Si OPAs are promising alternatives to near-IR c-Si OPAs, but they both have limitations in broadband operation.**

***Index Terms*—Amorphous silicon, mid-infrared, noise figure, optical parametric amplifiers, silicon photonics.**

I. Introduction

THE strong third-order optical nonlinearity of silicon makes silicon-on-insulator (SOI) waveguides a competitive platform for integrated nonlinear photonics [1]. There has been significant progress in the development of silicon-based active devices such as Raman-based optical amplifiers and lasers [2], as well as optical parametric amplifiers and wavelength converters based on the Kerr effect [3]. However, significant nonlinear loss mechanisms, i.e., TPA and FCA caused by the high optical intensities required for nonlinear interactions, have limited the performance and efficiency of these nonlinear devices [4]. Several methods have been proposed to mitigate this drawback. First, active carrier sweep-out using p-n junction diodes and short-pulse pumping can partially reduce FCA [5]; second, silicon photonics has been pursued in the mid-IR regime using optical pumps at wavelengths above the TPA threshold wavelength of 2.2 μm [6]. Silicon-on-sapphire (SOS) waveguides at 4.5 μm [7], SOS gratings couplers at 2.75 μm [8], silicon-on-nitride (SON) waveguides at 3.39 μm [9], optical Raman amplification at 3.4 μm [10], four-wave mixing (FWM) and parametric amplification at ∼2.2 μm [11] are some of the recent developments in the emerging field of mid-IR silicon photonics; Third, a-Si has shown promise for large parametric amplification and efficient wavelength conversion due to its large nonlinear figure of merit (FOM $= n_2/\beta_{\mathrm{TPA}}\lambda$, where β_{TPA} is the TPA coefficient and n_2 is the nonlinear refractive index) at telecom wavelengths [12]. Nonlinear coefficient as large as 2000 $(\mathrm{W.m})^{-1}$ [13] and FOM of ∼5, which is more than seven times higher than that of the SOI waveguides [14] are reported. Material degradation due to pump exposure used to limit the performance, however, optical stability has been greatly improved recently and no degradation of the nonlinear parameters was observed at peak pump intensity as high as 2 GW/cm^2 [14]. FWM gain of 26.5 dB [15] and conversion efficiency of 12 dB [16] have been demonstrated experimentally in hydrogenated a-Si nanowires.

One of the main concerns in the design of nonlinear photonic devices is the NF, which impairs the device performance. Several studies on the noise characteristics of silicon Raman amplifiers [17], [18], silicon Raman lasers [19], [20], and near-IR c-Si OPAs [21] have been reported. The signal-to-noise ratio (SNR) of mid-IR c-Si parametric wavelength converters has been studied in Ref. [22]. However, the noise originating from the pump lasers was excluded from the calculations and the waveguide was assumed to be lossless. This paper aims at full characterization of the signal NF spectrum in both near-IR a-Si and mid-IR c-Si OPAs. Main noise sources, i.e., photon fluctuations due to gain and loss in the medium and pump transferred noise (PTN), are accounted for and numerically simulated.

Specifically, the following aspects of a-Si and mid-IR c-Si OPAs are studied here for the first time. First, a-Si has a broadband Raman spectrum centered at 480 cm^{-1} (∼14.4 THz) [23]. The effect of the complex Raman nonlinearity on the process of FWM cannot be ignored in the analysis of gain and NF of a-Si OPAs. Second, unlike near-IR c-Si OPAs, in which the pump laser's RIN is not as effective as the ASE of the EDFA, mid-IR c-Si OPAs are usually pumped with optical parametric oscillators (OPOs) or high power pulsed lasers (e.g., Er:YAG lasers) instead of EDFA. Therefore, pump ASE noise does not exist but the RIN of the pump laser will be transferred to the signal and the final NF of the amplifier will be increased. Thus, the PTN must be analyzed using a different numerical model.

Manuscript received June 27, 2013; revised August 27, 2013; accepted August 27, 2013. Date of publication August 29, 2013; date of current version September 20, 2013. This work was supported by the United States' National Science Foundation CAREER Program under Award ECCS-1150672.

The authors are with the CREOL, The College of Optics and Photonics, University of Central Florida, Orlando, FL 32816 USA (e-mail: mjichi@creol.ucf.edu; fathpour@creol.ucf.edu).

Color versions of one or more of the figures in this paper are available online at http://ieeexplore.ieee.org.

Digital Object Identifier 10.1109/JLT.2013.2280213

0733-8724 © 2013 IEEE

II. Methodology

A. Near-IR a-Si OPAs

Unlike c-Si whose Raman spectrum peaks at a frequency shift of 15.6 THz and has a full-width at half-maximum (FWHM) of only 105 GHz [1], a-Si is less orderly in its atomic arrangement, and hence, has a broad Raman band centered at 14.4 THz [23]. When high pump power and large gain bandwidth are considered, the effect of Raman nonlinearity on the parametric amplification process becomes nonnegligible. Both the gain and NF spectra will be modified due to the complex Raman susceptibility. Raman-induced quantum-limited NF and asymmetric pump noise transfer in fiber OPAs have been analytically studied [24]. However, in a-Si OPAs, where nonlinear losses (TPA and FCA) are present, achieving accurate analytical solutions becomes difficult, if not impossible. In this paper, the impact of Raman nonlinear susceptibility on the performance of near-IR a-Si OPAs is investigated for the first time.

In previous studies of c-Si OPAs, the conventional nonlinear parameter $\gamma_0 = 2\pi n_2/A_{\rm eff}\lambda_p$ is always assumed to be constant over the telecommunication band (where λ_p is the pump wavelength and $A_{\rm eff}$ is the effective waveguide area). Here, a frequency dependent nonlinear parameter is defined:

$$\gamma(\Omega) = 2\pi n_2(\Omega)/\lambda_p A_{\rm eff} \tag{1}$$

where $n_2(\Omega) = 3\chi^{(3)}(\Omega)/(4\varepsilon_0 n_0^2 c)$ is the frequency dependent nonlinear refractive index (ε_0 is the permittivity of free space and c is the speed of light). The third-order susceptibility $\chi^{(3)}(\Omega)$ is composed of the nonresonant (or electronic) susceptibility $\chi^{(3)}_{\rm NR}$, which is a delta function in the time domain and a constant in the frequency domain, and the resonant (or Raman) susceptibility $\chi^{(3)}_R(\Omega)$, which is a time-delayed response and varies over the bandwidth of interest [24].

The real part of the Kerr nonlinearity in a-Si:H waveguides can be found in published measurements [13]. It should be noted that the γ reported in this reference is the sum of the nonresonant nonlinearity and the resonant nonlinearity at zero frequency shift. The broadband Raman gain profile $g_R(\Omega)$ of a-Si is previously characterized too [23]. Its maximum value is estimated to be ~4.735 cm/GW from Fig. 1 of Ref. [23], given the Raman gain coefficient of c-Si at wavelength of 1550 nm (20 cm/GW). The imaginary part of $\gamma(\Omega)$ equals to $g_R(\Omega)/2$ if the pump and the signal waves are copropagating and copolarized [24]. The real part of $\gamma(\Omega)$ is then calculated using Kramers–Kronig transformation for the parallel Raman susceptibility [25]:

$$\mathrm{Re}[\chi^{(3)}_R(\Omega)] = \frac{1}{\pi} P \int_{-\infty}^{\infty} d\Omega' \frac{\mathrm{Im}[\chi^{(3)}_R(\Omega')]}{\Omega' - \Omega} \tag{2}$$

where P denotes the principle part of the integral and is estimated to be 1.0203 in the case of a-Si. Fig. 1 shows the real and imaginary part of $\gamma(\Omega)$ of the waveguide studied later in Section III, including the Raman contribution. Assuming the pump intensity is much higher than the signal intensity, the coupled-mode equations that describe the evolution of the pump, signal, and idler amplitudes along the waveguide including the effect of the Raman susceptibility are as follows [26]:

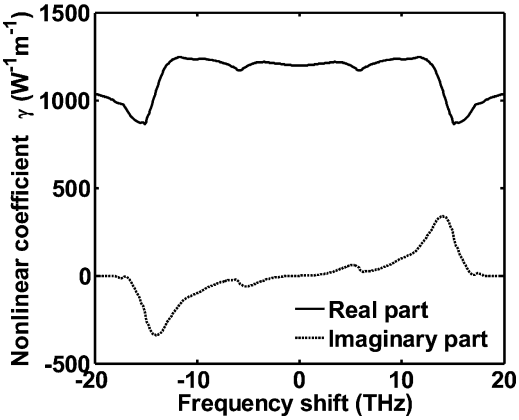

Fig. 1. Real and imaginary part of the nonlinear coefficient $\gamma(\Omega)$ including the Raman contribution. The effective area of the waveguide is assumed to be 0.07 μm^2.

$$\begin{aligned} dA_p/dz = &-1/2\left(\alpha + \alpha_p^{\rm FCA}(z)\right) A_p \\ &+ i\left(\gamma_0 + i\beta_{\rm TPA}/(2A_{\rm eff})\right)|A_p|^2 A_p \end{aligned} \tag{3a}$$

$$\begin{aligned} dA_s/dz = &-1/2\left(\alpha + \alpha_s^{\rm FCA}(z)\right) A_s \\ &+ i\left(\gamma_0 + \gamma(-\Omega) + i\beta_{\rm TPA}/A_{\rm eff}\right)|A_p|^2 A_s \\ &+ i\gamma(-\Omega) A_p^2 A_i^* \exp(-i\Delta k z) \end{aligned} \tag{3b}$$

$$\begin{aligned} dA_i/dz = &-1/2\left(\alpha + \alpha_i^{\rm FCA}(z)\right) A_i \\ &+ i\left(\gamma_0 + \gamma(\Omega) + i\beta_{\rm TPA}/A_{\rm eff}\right)|A_p|^2 A_i \\ &+ i\gamma(\Omega) A_p^2 A_s^* \exp(-i\Delta k z). \end{aligned} \tag{3c}$$

Here, α is the linear loss of the waveguide, $\beta_{\rm TPA}$ is the TPA coefficient, A_j is the field amplitude of the three waves in unit of W$^{1/2}$, and $\alpha_j^{\rm FCA}(z) = 1.45 \times 10^{-17}(\lambda_j/1.55)^2 \tau_{\rm eff}\beta_{\rm TPA}|A_p|^4/(2E_p A_{\rm eff}^2)$, where $\tau_{\rm eff}$ is the effective carrier lifetime, and E_p is the photon energy at pump wavelength ($j = p, s, i$). $\Omega = \omega_i - \omega_p = \omega_p - \omega_s$ is the frequency deviation from the pump wavelength. $\Delta k = k_s + k_i - 2k_p = \beta_2\Omega^2$ is the phase mismatch between the three waves, where k_j is the propagation constant at frequency ω_j and β_2 is the group velocity dispersion coefficient.

To estimate the total NF of silicon OPAs, the noise induced by photon fluctuations in the material and the noise induced by the noise of the pump sources are calculated separately. In the presence of nonlinear TPA and FCA losses, the above coupled-mode equations do not have analytical solutions as in optical fibers. Therefore, the model in Ref. [24] cannot be applied to a-Si OPAs. Here, the noise model in [17] and [21] for linear optical amplifiers is used. The analysis of noise in a-Si OPAs is more complicated than that of c-Si OPAs due to the frequency dependent nonlinear coefficient. The coupled-mode equations are first solved numerically. The numerical solutions, i.e., the distribution of the three waves along the a-Si waveguide (z-direction) are then used to calculate the photon number fluctuations

induced by gain and loss in the FWM process:

$$N_g = \int_0^L g(z) \exp\left(\int_z^L [g(z') - \gamma'(z')]dz'\right)dz \quad (4a)$$

$$N_i = \int_0^L \gamma'(z) \exp\left(\int_z^L [g(z') - \gamma'(z')]dz'\right)dz \quad (4b)$$

where $g(z)$ and $\gamma'(z)$ are gain and loss parameters, respectively. Assuming the input photon number at the signal wavelength is large enough, the NF induced by photon fluctuations can be calculated as [17], [21]:

$$NF_{\rm pf} = (N_o + N_g + N_l)/N_o \quad (5)$$

where N_o is the mean output photon number.

At near-IR, an EDFA is usually used as the pump source. The ASE noise of the EDFA is transferred to the signal during the parametric amplification process. The RIN of the pump laser (before getting amplified by the EDFA) can also impact the performance of the a-Si OPA. However, the availability of low noise lasers at telecom wavelength with RIN below -160 dB/Hz makes the contribution of pump-to-signal RIN transfer negligible. The case for mid-IR OPAs is completely different, as will be discussed in the Section II-B. To calculate the signal variation due to the power variation of the input pump $\Delta P_{\rm pin}$, the output signal $P_{\rm sout} = |A_s\ (z = L)|^2$ is assumed to be linearly dependent on the mean input pump power $P_{\rm pin} = |A_p(z = 0)|^2$, if $\Delta P_{\rm pin}$ is small. Consequently, the quadratic fluctuation terms can be neglected:

$$P_{\rm sout}(P_{\rm pin}) = G(P_{\rm pin}) \cdot P_s(z = 0) + B \cdot \Delta P_{\rm pin} \quad (6)$$

where $G(P_{\rm pin})$ is the signal gain as a function of input pump power, and B is the slope of $P_{\rm sout}$ at $P_{\rm pin}$. The analytical expression of B can be found in Ref. [27] for lossless waveguides. However, B must be calculated numerically in a-Si waveguides due to the presence of linear and nonlinear losses. If the quantum noise of the pump source as well as the ASE-ASE beating terms are neglected and only the pump-ASE beating noise is considered, the linear NF increase (after detection) contributed by the noisy pump is given by [27]:

$$\Delta NF_{\rm pump} = \frac{2B^2 P_{\rm pin} n_{sp}(G_A - 1)}{G(P_{\rm pin})^2 P_s(z = 0)} \quad (7)$$

where n_{sp} is the population inversion factor of the EDFA and G_A is the gain of the EDFA. It is noticed that B is proportional to P_s $(z = 0)$, therefore, $\Delta NF_{\rm pump}$ is linearly dependent on the input signal power, while $\Delta NF_{\rm pf}$ does not have signal dependence. The total NF of a-Si OPAs is finally obtained by

$$NF = NF_{\rm pf} + \Delta NF_{\rm pump}. \quad (8)$$

B. Mid-IR c-Si OPAs

TPA and FCA vanish in the mid-IR regime in c-Si. Although three-photon absorption (3PA) and associated free-carrier effects are considerable for pump intensities of a few GW/cm^2 in the wavelength range of 2300–3300 nm [28], [29], in our case, the pump laser wavelength is assumed to be 3.4 μm. Since this pump photon energy is below one third of silicon's indirect bandgap, 3PA-induced nonlinear losses are negligible for small signal intensities. Also, although the Kerr effect is weaker in the mid-IR, and the larger λ further reduces the conventional nonlinear parameter γ, FWM on SOI waveguides perform better at $\sim$2.2 μm when compared to $\sim$1.5 μm due to lower nonlinear losses [11]. $n_2 = 1 \times 10^{-5}$ cm^2/GW was measured at 2.35 μm [30] and theoretical calculations were published that predict different n_2 values (3.67 to 3.26 $\times$ 10^{-5} cm^2/GW for λ varying from 3.39 to 4.26 μm [31]). The latter are the values used in this study.

Noise sources in mid-IR c-Si OPAs are similar to those in a-Si OPAs. Modeling of photon fluctuations in mid-IR c-Si OPAs is much easier because $\beta_{\rm TPA}$, $\alpha_j^{\rm FCA}(z)$, and $\lambda(\pm\Omega)$ in Eqs. (3a)–(3c) can be simply set to be zero. The nonlinear coefficient λ is assumed to be real and constant over the frequency range of interest because the Raman gain spectrum of c-Si has a sharp peak at a frequency shift of 15.6 THz and the common bandwidth of c-Si OPAs is only a few terahertz. However, the PTN of mid-IR c-Si OPAs should be modeled differently because mid-IR optical amplifiers are not commercially available. Mid-IR high power sources such as pulsed lasers and OPOs have low beam quality and high intensity fluctuations. Therefore, the RIN transferred from pump to signal should be analyzed instead of the ASE noise of the pump.

The noise component at angular frequency ω in the pump noise spectrum is considered. A sinusoidal noise term is introduced on the pump, signal, and idler amplitudes:

$$A_j(z,t) = \bar{A}_j(z) + \Delta A_j(z,t) = \bar{A}_j(z)[1 + \delta_j(z)\exp(i\omega t)] \quad (9)$$

where $\bar{A}_j(z)$ $(j = p, s, i)$ are time-independent average intensities, $\delta_j(z)$ are time-independent complex values that satisfy $|\delta_j(z)| \ll 1$. The different values of pump, signal, and idler group velocities, v_p, v_s, and v_i should be accounted for, especially for high modulation frequencies (>1 GHz). The coupled-mode equations including group velocities and neglecting nonlinear losses as well as Raman contribution are as follows:

$$\partial A_p/\partial z + 1/v_p \cdot \partial A_p/\partial t = -(1/2)\alpha A_p + i\gamma |A_p|^2 A_p \quad (10a)$$

$$\partial A_s/\partial z + 1/v_s \cdot \partial A_s/\partial t = -(1/2)\alpha A_s + 2i\gamma |A_p|^2 A_s + i\gamma A_i^* A_p^2 \exp(-i\Delta k z) \quad (10b)$$

$$\partial A_i/\partial z + 1/v_i \cdot \partial A_i/\partial t = -(1/2)\alpha A_i + 2i\gamma |A_p|^2 A_i + i\gamma A_s^* A_p^2 \exp(-i\Delta k z). \quad (10c)$$

Substituting Eq. (9) into Eq. (10) and neglecting higher order fluctuation terms, the propagation equations for the pump, signal and idler amplitude modulations are obtained:

$$\partial \Delta A_p/\partial z = -i\omega \Delta A_p/v_p - (1/2)\alpha \Delta A_p + i\gamma(2|\bar{A}_p|^2 \Delta A_p + \bar{A}_p^2 \Delta A_p^*) \quad (11a)$$

TABLE I
SUMMARY OF LINEAR AND NONLINEAR OPTICAL PROPERTIES OF THREE DIFFERENT TYPES OF SILICON WAVEGUIDES

	c-Si (near-IR)	a-Si (near-IR)	c-Si (mid-IR)
n_2 (m^2/W)	5.5×10^{-18}	2.1×10^{-17}	3.67×10^{-18}
α (dB/cm)	< 0.2	> 2	~ 1
β_{TPA} (cm/GW)	0.7	0.25	--
τ_{eff}	~ ns	~ ps	--
FOM	0.3-0.5	~ 5	--

$$\partial\Delta A_s/\partial z = -i\omega\Delta A_s/v_s - (1/2)\alpha\Delta A_s + 2i\gamma(\left|\bar{A}_p\right|^2\Delta A_s + \bar{A}_p\bar{A}_s\Delta A_p^* + \bar{A}_p^*\bar{A}_s\Delta A_p) + i\gamma(\bar{A}_p^2\Delta A_i^* + 2\bar{A}_p\bar{A}_i^*\Delta A_p)\exp(-i\Delta kz) \quad (11b)$$

$$\partial\Delta A_i/\partial z = -i\omega\Delta A_i/v_i - (1/2)\alpha\Delta A_i + 2i\gamma(\left|\bar{A}_p\right|^2\Delta A_i + \bar{A}_p\bar{A}_i\Delta A_p^* + \bar{A}_p^*\bar{A}_i\Delta A_p) + i\gamma(\bar{A}_p^2\Delta A_s^* + 2\bar{A}_p\bar{A}_s^*\Delta A_p)\exp(-i\Delta kz). \quad (11c)$$

The RIN transfer is then calculated as the ratio of the signal RIN at the output of the OPA and the pump RIN at the input of the OPA:

$$T_{\mathrm{RIN}} = \left(\frac{\Delta P_s(L)}{\bar{P}_s(L)}\right)^2 \Big/ \left(\frac{\Delta P_p(0)}{\bar{P}_p(0)}\right)^2 = \frac{\left(\bar{A}_s^*(L)\Delta A_s(L) + \bar{A}_s(L)\Delta A_s^*(L)\right)^2\left|\bar{A}_p(0)\right|^2}{\left(\bar{A}_p^*(0)\Delta A_p(0) + \bar{A}_p(0)\Delta A_p^*(0)\right)^2\left|\bar{A}_s(L)\right|^2}. \quad (12)$$

The linear NF increase due to pump-to-signal RIN transfer is given by [18]:

$$\Delta NF_{\mathrm{pump}} = RIN_{\mathrm{pump}}T_{\mathrm{RIN}}\bar{P}_s(0)\lambda_s/2hc \quad (13)$$

where h is the Planck's constant. Similar to near-IR a-Si OPAs, the PTN contribution to the total NF is also linearly dependent on the input signal power.

III. RESULTS AND DISCUSSION

A. Near-IR a-Si OPAs

Table I summarizes the linear and nonlinear optical properties of near-IR c-Si, near-IR a-Si, and mid-IR c-Si waveguides employed in this study. It is noted that, unlike c-Si, the nonlinear optical properties of a-Si:H such as β_{TPA} and $\gamma(\Omega)$ strongly depend on the fabrication process, i.e., its composition (hydrogen content) or atomic arrangement. γ_0 as high as 2000 $\mathrm{W^{-1}m^{-1}}$ [14] and β_{TPA} as low as 0.08 cm/GW [32] have been reported for a-Si waveguides. However, unfortunately they cannot be achieved simultaneously. Nonlinear parameters $\gamma_0 = 1200\,\mathrm{W^{-1}m^{-1}}$ and $\beta_{\mathrm{TPA}} = 0.25$ cm/GW [13] are used in the following simulations as they provide the highest nonlinear FOM (~5) reported to date. The studied waveguides are 500 nm wide and 220 nm high and have an effective area $A_{\mathrm{eff}} = 0.07\ \mu\mathrm{m}^2$. The length of the devices is 2 cm. The group velocity dispersion (GVD) of the waveguides is set to be 200 $\mathrm{ps.km^{-1}.nm^{-1}}$,

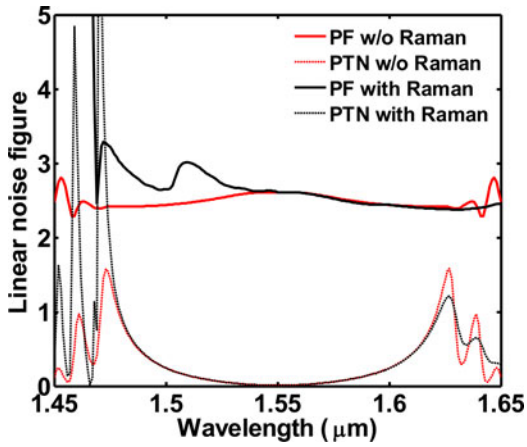

Fig. 2. Linear NF spectra of near-IR a-Si OPA pumped at wavelength of 1550 nm with a peak intensity of 500 $\mathrm{MW/cm^2}$. The noise sources contribute to the total NF, i.e., photon fluctuations and PTN are modeled separately. For the NF spectra calculation excluding the Raman effect (dashed lines), $\mathrm{Im}\{\gamma(\Omega)\} = 0$. The linear loss of the waveguide is 2 dB/cm.

which leads to a large gain bandwidth of >200 μm (see Fig. 3), and thus, more apparent Raman-induced noise. Although the linear loss of a-Si waveguides are higher than c-Si waveguides, the propagation losses as low as 3.2 ± 0.2 dB/cm for the TE mode and 2.3 ± 0.1 dB/cm for the TM mode have been reported for submicron (200 nm × 500 nm) a-Si wire waveguides [33]. Free-carrier lifetimes in the picosecond range have been measured [34]. Here, the devices are assumed to be pumped with a peak intensity of 500 $\mathrm{MW/cm^2}$ at wavelength of 1550 nm. In the simulation of PTN contribution to the NF, $n_{sp} = 1.5$ and $G_A = 50$ are used as typical near-IR lasers have 1–10 mW of output power before amplification. The input signal power is assumed to be 10 μW.

Fig. 2 shows the linear NF spectrum of a-Si OPA pumped at 1550 nm. The NF spectrum without Raman effect, i.e., $\gamma(\Omega) = \gamma_0$ or $\mathrm{Im}\{\gamma(\Omega)\} = 0$, is also plotted for comparison. As illustrated, the NF contribution from gain and loss fluctuations is greater than the PTN contribution so that it can be treated as the dominant noise source in a-Si OPAs, when the input signal power is small. It is shown that when the Raman effect is taken into account, the NF spectra for both gain and loss fluctuations and PTN become asymmetric due to the real and imaginary part of the Raman susceptibility. For signal wavelengths that are longer than the pump wavelength (Stokes side or negative frequency shift), the NF spectrum are slightly modified when Raman-induced noise is considered. For signal wavelengths shorter than the pump wavelength (anti-Stokes side or positive frequency shift), the NF is evidently increased compared to the NF without Raman, especially at the gain edge (see Fig. 3). Similar results have been obtained in lossless fiber OPAs [24]. In this paper, for the first time, linear and nonlinear losses, as well as the complex third order susceptibility are all considered at the same time.

In Fig. 3, the gain and total NF spectra are plotted in logarithmic scale. For linear loss as low as 2 dB/cm, wideband optical gain (maximum 30 dB) is obtained with a NF of ~5 dB at wavelengths from 1.48 to 1.65 μm. The asymmetry of the

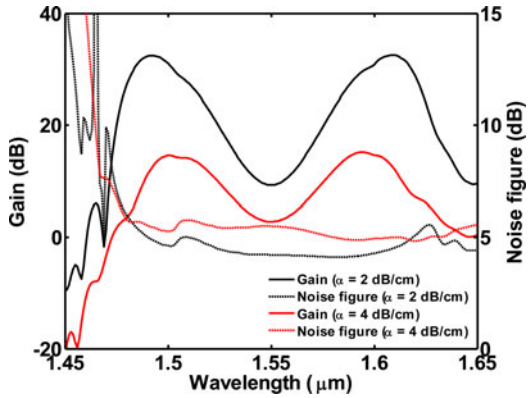

Fig. 3. Gain and total NF spectra of near-IR a-Si OPAs with linear propagation losses of 2 and 4 dB/cm. Raman susceptibility is included.

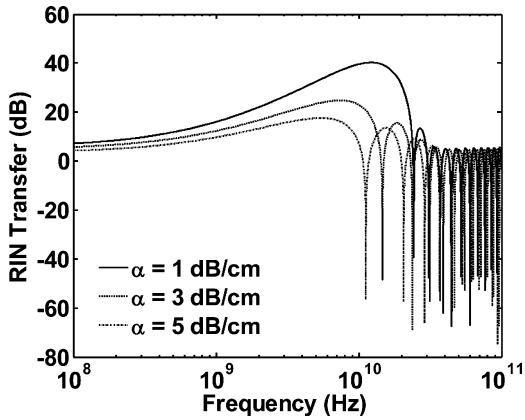

Fig. 4. Pump-to-signal RIN transfer spectra for mid-IR c-Si OPAs with linear propagation losses of 1, 3, and 5 dB/cm. The OPA is pumped at a wavelength of 3.4 μm with a peak intensity of 3 GW/cm^2.

gain spectrum is obvious due to the Raman gain on the Stokes side and Raman loss on the anti-Stokes side. The NF increases sharply to above 20 dB at the gain edge on the anti-Stokes side. Although the gain at wavelengths $\sim$1.47 μm is still high (10 dB or more), the overall performance of the OPA is poor because of the high NF. Therefore, operation of the a-Si OPA is limited by the NF for signal frequencies larger than the pump frequency. Linear loss of 4 dB/cm is also considered because low linear loss and high nonlinear FOM may not be achieved simultaneously. It is clear that for OPAs with higher propagation loss, the gain is lower and the NF is slightly higher over the gain bandwidth.

B. Mid-IR c-Si OPAs

In order to satisfy the phase matching condition required by OPAs, an SOS waveguide is designed by dispersion engineering to achieve wideband anomalous dispersion ($D > 0$). The SOS waveguide is 1.5 μm wide and 0.5 μm high and exhibits D of 250– 450 ps.km^{-1}.nm^{-1} in the wavelength range of 2.9–3.9 μm. The pump wavelength is fixed at 3.4 μm. Due to the absence of nonlinear losses, increasing the pump power will always increase the gain of the OPA. The limiting factor, therefore, becomes the damaging threshold of silicon instead of the pump depletion due to FCA. Optical gain of $\sim$30 dB is easily obtained at a peak pump intensity of 3 GW/cm^2 assuming the waveguide linear loss is 1 dB/cm and the length of the waveguide is 3 cm [see Fig. 6(a)].

Fig. 4 presents the modulation frequency dependent pump-to-signal RIN transfer for waveguide losses of 1, 3, and 5 dB/cm at the wavelength of 3.338 μm, where the gain peaks [see Fig. 6(a)]. RIN transfer remains constant at low frequencies, and then starts to oscillate at $>$10 GHz. The observed strong oscillations at higher frequencies suggest that laser sources with RIN spectra not wider than 10 GHz are required for pumping mid-IR c-Si OPAs. The RIN values of the signal at lower frequencies could be about 5$\sim$10 dB higher than that of the pump for waveguide with linear loss of 5 dB/cm, and the situation is even worse for waveguides with lower propagation losses (larger parametric gain).

Fig. 5(a) and (b) presents the linear NF spectrum of mid-IR c-Si OPAs for propagation losses of 1 dB/cm and 3 dB/cm,

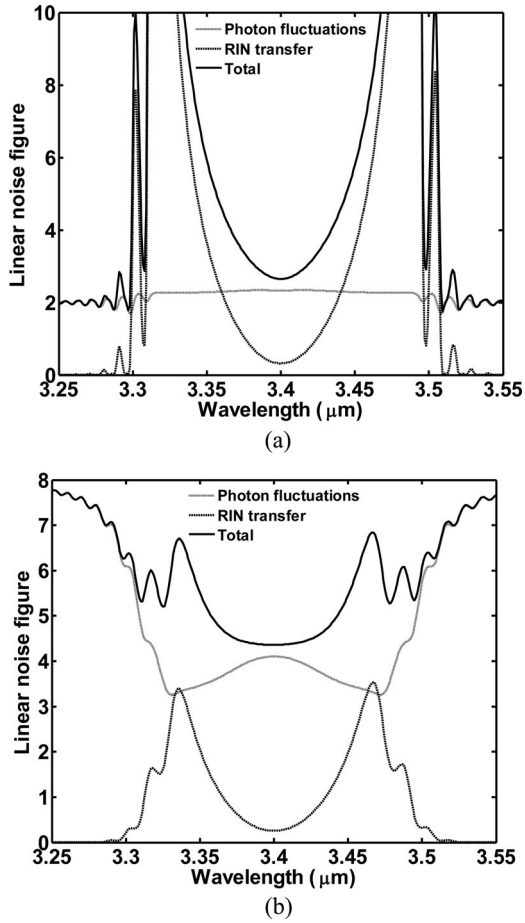

Fig. 5. Linear NF spectra of mid-IR c-Si OPAs pumped at wavelength of 3.4 μm with a peak intensity of 3 GW/cm^2. The noise sources contribute to the total NF, i.e., photon fluctuations and RIN transfer are modeled separately: (a) $\alpha = 1$ dB/cm and (b) $\alpha = 3$ dB/cm.

respectively. Noise sources including gain and loss fluctuations and low-frequency pump-to-signal RIN transfer are both taken into account. No data on the RIN of mid-IR lasers is currently available. The pump RIN used in the following simulations is –140 dB/Hz, assuming mid-IR OPOs or pulsed lasers have similar

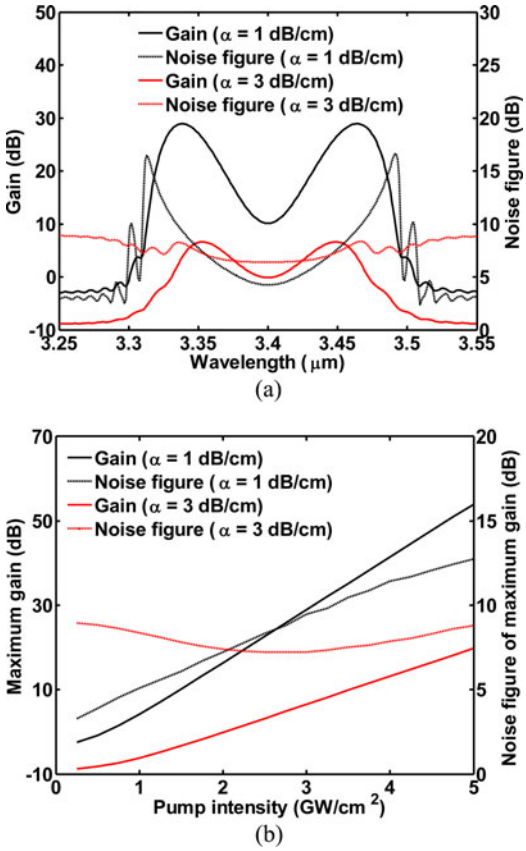

Fig. 6. (a) Gain and total NF spectra of mid-IR c-Si OPAs with linear propagation losses of 1 dB/cm and 3 dB/cm; and (b) NF evolution at the maximum gain.

noise performance as typical near-IR pump lasers, whose RIN is 20 dB worse than near-IR lasers used in optical communications [18]. It is evident that for mid-IR c-Si OPA with linear loss of 1 dB/cm [see Fig. 5 (a)], the noise induced by photon fluctuations is just slightly above the well-known 3 dB NF limit for an ideal OPA, while the noise transferred from the pump source is much higher, which leads to a total NF of well above 10 dB at the gain edge [see Fig. 6(a)]. In OPAs with linear loss of 3 dB/cm [see Fig. 5(b)], the pump-to-signal RIN transfer dominates over the noise induced by gain and loss fluctuations. In Fig. 6(a), the gain and NF spectra of the mid-IR c-Si OPAs are plotted in logarithmic scale. Unlike near-IR a-Si OPAs, in which higher amplification always leads to lower NF, in mid-IR c-Si OPAs, the gain and NF are both higher for lower propagation loss at large frequency shift (around the maximum gain). This is because the RIN transfer increases with increasing gain as illustrated in Fig. 4. This limits the performance of low-loss mid-IR c-Si OPAs for large bandwidth operation. In Fig. 6(b), the maximum gain and NF of maximum gain are plotted versus peak pump intensity. It is shown that there is no gain saturation as in near-IR c-Si OPAs [21] because of the absence of TPA and FCA. For linear noise of 1 dB/cm, the NF of maximum gain keeps increasing when the pump intensity increases due to the high pump-to-signal RIN transfer which is the dominant noise source. For linear loss of 3 dB/cm, the noise figure of maximum gain is almost constant ($<$10 dB) for pump intensities ranging from a few hundred MW/cm^2 to 5 GW/cm^2. This originates from the mutual influence of photon fluctuations (which decreases with increasing pump intensity) and pump-to-signal RIN transfer (which increases with increasing pump intensity).

The gain and NF spectra of near-IR a-Si OPAs (see Fig. 3) and mid-IR c-Si OPAs [see Fig. 6(a)] are quite different from those of near-IR c-Si OPAs previously studied in Ref. [21]. Near-IR c-Si OPAs pumped with pulsed lasers have a maximum gain of $\sim$10 dB, even when the carrier sweep-out technique is applied. Further increasing the pump power will result in lower gain and higher NF at the same time due to the intensity-dependent nonlinear losses. In contrast, in near-IR a-Si OPAs and mid-IR c-Si OPAs, $>$30 dB gain can be easily achieved and no saturation of the gain is observed with pump intensity up to a few GW/cm^2. Slight asymmetry appears in the gain spectrum of a-Si OPAs due to the Raman-effect-induced gain and loss. The NF spectrum of near-IR c-Si OPAs ([21], Fig. 3) is more or less symmetric with respect to the pump wavelength (slight asymmetry comes from the wavelength dependence of FCA). The NF is around 10 dB for small frequency detuning and drops to below 6 dB at the gain edge. However, in near-IR a-Si OPAs, the NF is only about 5 dB on the Stokes side due to the low nonlinear losses, but increases sharply at the gain edge on the anti-Stokes side. The NF spectrum of mid-IR c-Si OPA is strictly symmetric with respect to the pump wavelength. However, unlike near-IR c-Si OPAs in which gain and loss fluctuations is the dominant noise source, the NF of mid-IR c-Si OPAs might be dominated by the pump-to-signal RIN transfer. Large gain and small NF cannot be achieved at the same time because the RIN transfer increases with increasing gain.

IV. Conclusion

In this paper, the NF spectra of near-IR a-Si OPAs and mid-IR c-Si OPAs are investigated theoretically. Noise sources including gain and loss fluctuations and PTN are both considered. The Raman-effect-induced complex nonlinear coefficient, which in principle comes from the nonzero response time of $\chi^{(3)}$, should be taken into account in a-Si OPAs, as it induces asymmetry in the gain and NF spectra. ASE noise of EDFA and RIN transfer from OPOs or pulsed lasers are recognized as the main contribution to the PTN in near-IR a-Si OPAs and mid-IR c-Si OPAs, respectively. It is shown that in near-IR a-Si OPAs, the NF is dominated by gain and loss fluctuations if input signal power is small. The NF is $\sim$5 dB on the Stokes side but becomes large at the gain edge on the anti-Stokes side. In mid-IR c-Si OPAs, the NF might be dominated by the pump-to-signal RIN transfer when the propagation loss of the waveguide is low (1 dB/cm) and the optical gain of the amplifier is high. The NF is above 10 dB around the wavelength where the maximum gain is achieved. In summary, near-IR a-Si OPAs and mid-IR c-Si OPAs are both excellent candidates for large parametric amplification ($>$30 dB gain with a reasonable pump intensity) and promising alternatives to near-IR c-Si OPAs, which suffers from TPA and FCA. However, they both have limitations in

broadband operation due to Raman-effect induced asymmetric NF spectrum and pump-to-signal RIN transfer, respectively.

REFERENCES

[1] J. Leuthold, C. Koos, and W. Freude, "Nonlinear silicon photonics," *Nature Photon.*, vol. 4, pp. 535–543, 2010.

[2] A. Liu, H. Rong, R. Jones, O. Cohen, D. Hak, and M. Paniccia, "Optical amplification and lasing by stimulated Raman scattering in silicon waveguides," *J. Lightw. Technol.*, vol. 24, no. 3, pp. 1440–1455, Mar. 2006.

[3] K. K. Tsia, S. Fathpour, and B. Jalali, "Energy harvesting in silicon wavelength converters," *Opt. Exp.*, vol. 14, pp. 12327–12333, 2006.

[4] R. Claps, V. Raghunathan, D. Dimitropoulos, and B. Jalali, "Influence of nonlinear absorption on Raman amplification in Silicon waveguides," *Opt. Exp.*, vol. 12, pp. 2774–2780, 2004.

[5] H. Rong, R. Jones, A. Liu, O. Cohen, D. Hak, A. Fang, and M. Paniccia, "A continuous-wave Raman silicon laser," *Nature*, vol. 433, pp. 725–728, 2005.

[6] B. Jalali, V. Raghunathan, R. Shori, S. Fathpour, D. Dimitropoulos, and O. Stafsudd, "Prospects for silicon mid-IR Raman lasers," *IEEE J. Sel. Top. Quantum Electron.*, vol. 12, no. 6, pp. 1618–1627, Nov./Dec. 2006.

[7] T. Baehr-Jones, A. Spott, R. Ilic, B. Penkov, W. Asher, and M. Hochberg, "Silicon-on-sapphire integrated waveguides for the mid-infrared," *Opt. Exp.*, vol. 18, pp. 12127–12135, 2010.

[8] Z. Cheng, X. Chen, C. Y. Wong, K. Xu, C. K. Y. Fung, Y. M. Chen, and H. K. Tsang, "Mid-infrared grating couplers for silicon-on-sapphire waveguides," *IEEE Photon. J.*, vol. 4, no. 1, pp. 104–113, Feb. 2012.

[9] S. Khan, J. Chiles, J. Ma, and S. Fathpour, "Silicon-on-nitride waveguides for mid- and near-infrared integrated photonics," *Appl. Phys. Lett.*, vol. 102, p. 121104, 2013.

[10] V. Raghunathan, D. Borlaug, R. R. Rice, and B. Jalali, "Demonstration of a mid-infrared silicon Raman amplifier," *Opt. Exp.*, vol. 15, pp. 14355–14362, 2007.

[11] X. Liu, R. M. Osgood, Y. A. Vlasov, and W. M. J. Green, "Mid-infrared optical parametric amplifier using silicon nanophotonic waveguides," *Nature Photon*, vol. 4, pp. 557–560, 2010.

[12] Y. Okawachi, A. L. Gaeta, and M. Lipson, "Breakthroughs in nonlinear silicon photonics 2011," *IEEE. Photon. J.*, vol. 4, no. 2, pp. 601–605, Oct. 2012.

[13] C. Grillet, L. Carletti, C. Monat, P. Grosse, B. B. Baker, S. Menezo, J. M. Fedeli, and D. J. Moss, "Amorphous silicon nanowires combining high nonlinearity, FOM and optical stability," *Opt. Exp.*, vol. 20, pp. 22609–22615, 2012.

[14] K. Narayanan and S. F. Preble, "Optical nonlinearities in hydrogenated-amorphous silicon waveguides," *Opt. Exp.*, vol. 18, pp. 8998–9005, 2010.

[15] B. Kuyken, S. Clemmen, S. K. Selvaraja, W. Bogaerts, D. V. Thourhout, P. Emplit, S. Massar, G. Roelkens, and R. Baets, "On-chip parametric amplification with 26.5 dB gain at telecommunication wavelengths using CMOS-compatible hydrogenated amorphous silicon waveguides," *Opt. Lett.*, vol. 36, pp. 552–554, 2011.

[16] B. Kuyken, H. Ji, S. Clemmen, S. K. Selvaraja, H. Hu, M. Pu, M. Galili, P. Jeppesen, G. Morthier, S. Massar, L. K. Oxenlowe, G. Roelkens, and R. Baets, "Nonlinear properties of and nonlinear processing in hydrogenated amorphous silicon waveguides," *Opt. Exp.*, vol. 19, pp. B146–B153, 2011.

[17] D. Dimitropoulos, D. R. Solli, R. Claps, O. Boyraz, and B. Jalali, "Noise figure of silicon Raman amplifiers," *J. Lightw. Technol.*, vol. 26, no. 7, pp. 847–852, Apr. 2008.

[18] X. Sang, D. Dimitropoulos, and B. Jalali, "Influence of pump-to-signal RIN transfer on noise figure in silicon Raman amplifiers," *IEEE Photon. Technol. Lett.*, vol. 20, no. 24, pp. 2021–2023, Dec. 2008.

[19] J. Ma and S. Fathpour, "Pump-to-Stokes relative intensity noise transfer and analytical modeling of mid-infrared silicon Raman lasers," *Opt. Exp.*, vol. 20, pp. 17962–17972, 2012.

[20] X. Liu, X. Sang, B. Yan, K. Wang, C. Yu, and W. Dou, "Influences of pump-to-Stokes RIN transfer on the single-order silicon Raman lasers," *Optoelectron. Adv. Mater. Rapid Comm.*, vol. 4, pp. 1284–1288, 2010.

[21] X. Sang and O. Boyraz, "Gain and noise characteristics of high-bit-rate silicon parametric amplifiers," *Opt. Exp.*, vol. 16, pp. 13122–13132, 2008.

[22] Y. Huang, E. K. Tien, S. Gao, S. K. kalyoncu, Q. Song, F. Qian, E. Adas, D. Yildirim, and O. Boyraz, "Electrical signal-to-noise ratio improvement in indirect detection of mid-IR signals by wavelength conversion in silicon-on-sapphire waveguides," *Appl. Phys. Lett.*, vol. 99, p. 181122, 2011.

[23] T. Deschaines, J. Hodkiewicz, and P. Henson. (2009). Characterization of amorphous and microcrystalline silicon using Raman spectroscopy. [Online]. Available: http://www.thermoscientific.fr/eThermo/CMA/PDFs/Product/productPDF_56886.PDF

[24] P. L. Voss and P. Kumar, "Raman-effect induced noise limits on $\chi^{(3)}$ parametric amplifiers and wavelength converters," *J. Opt. B: Quantum Semiclass. Opt.*, vol. 6, pp. S762–S770, 2004.

[25] F. Bassani and S. Scandolo, "Dispersion relations and sum rules in nonlinear optics," *Phys. Rev. B*, vol. 44, pp. 8446–3453, 1991.

[26] E. Golovchenko, P. V. Mamyshev, A. N. Pilipetskii, and E. M. Dianov, "Mutual influence of the parametric effects and stimulated Raman scattering in optical fibers," *IEEE J. Quantum Electron.*, vol. 26, no. 10, pp. 1815–1820, Oct. 1990.

[27] P. Kylemark, P. O. Hedekvist, H. Sunnerud, M. Karlsson, and P. A. Andrekson, "Noise characteristics of fiber optical parametric amplifiers," *J. Lightw. Technol.*, vol. 22, no. 2, pp. 409–416, Feb. 2004.

[28] S. Pearl, N. Rotenberg, and H. M. Driel, "Three photon absorption in silicon for 2300–3300 nm," *Appl. Phys. Lett.*, vol. 93, p. 131102, 2008.

[29] Z. Wang, H. Liu, N. Huang, Q. Sun, J. Wei, and X. Li, "Influence of three-photon absorption on mid-infrared cross-phase modulation in silicon-on-sapphire wavegudies," *Opt. Exp.*, vol. 21, pp. 1840–1848, 2013.

[30] Q. Lin, J. Zhang, G. Piredda, R. W. Boyd, P. M. Fauchet, and G. P. Agrawal, "Dispersion of silicon nonlinearities in the near infrared region," *Appl. Phys. Lett.*, vol. 91, p. 021111, 2007.

[31] N. K. Hon, R. Soref, and B. Jalali, "The third-order nonlinear optical coefficients of Si, Ge, and Si1-xGex in the midwave and longwave infrared," *J. Appl. Phys.*, vol. 110, p. 011301, 2011.

[32] Y. Shoji, T. Ogasawara, T. Kamei, Y. Sakakibara, S. Suda, K. Kintaka, H. Kawashima, M. Okano, T. Hasama, H. Ishikawa, and M. Mori, "Ultrafast nonlinear effects in hydrogenated amorphous silicon wire waveguides," *Opt. Exp.*, vol. 18, pp. 5668–5673, 2010.

[33] S. Zhu, G. Q. Lo, and D. L. Kwong, "Low-loss amorphous silicon wire waveguide for integrated photonics: effect fabrication process and the thermal stability," *Opt. Exp.*, vol. 18, pp. 25283–25291, 2010.

[34] S. Suda, K. Tanizawa, Y. Sakakibara, T. Kamei, K. Nakanishi, E. Itoga, T. Ogasawara, R. Takei, H. Kawashima, S. Namiki, M. Mori, T. Hasama, and H. Ishikawa, "Pattern-effect-free all-optical wavelength conversion using a hydrogenated amorphous silicon waveguide with ultra-fast carrier decay," *Opt. Lett.*, vol. 37, pp. 1382–1384, 2012.

Jichi Ma is working toward the Ph.D. degree in optics at the University of Central Florida, Orlando, FL, USA. His research interests include nonlinear integrated photonics, silicon photonics, and mid-wave infrared optics.

Sasan Fathpour is an Assistant Professor at CREOL, The College of Optics and Photonics, University of Central Florida, Orlando, FL, USA. He has received the United States' National Science Foundation CAREER and Office of Naval Research Young Investigator Program awards. He is a coauthor of about 90 publications and is a Senior Member of IEEE, the OSA, and the SPIE.